CHARACTERIZATION OF AMD SEDIMENTS IN THE DISCHARGE OF THE TINTO SANTA ROSA MINE (IBERIAN PYRITIC BELT, SW SPAIN)

M.P. Asta[1], J. Cama[1], A.G. Gault[2], J.M. Charnock[2,3] and I. Queralt[1]

[1]*Institute of Earth Sciences "Jaume Almera", CSIC, c/Lluís Solé i Sabarís s/n, 08028 Barcelona, Spain.*
[2]*School of Earth, Atmospheric and Environmental Sciences and Williamson Research Centre for Molecular Environmental Science, University of Manchester, Oxford Road, Manchester, M13 9PL, UK*
[3]*CCLRC Daresbury Laboratory, Daresbury, Warrington, WA4 4AD, UK*

Abstract

The acidic discharge of the Tinto Santa Rosa mine in the Iberian Pyritic Belt (SW, Spain) transports high concentrations of acidity, sulfate and metal(loid)s (e.g., Fe, As, Co, Ni, Cu, Pb, and Mn). This study deals with the mobility of As in this stream, which appears to be associated with the sediments and precipitates of the stream floor. Characterization of the precipitates and sediments from the stream bed was performed by X-ray diffraction (XRD), X-ray-fluorescence (XRF), scanning electron microscopy (SEM) and X-ray absorption spectroscopy (XAS). The aqueous concentration of arsenic and iron decreases markedly from the adit mouth to 300 m downstream due to precipitation of iron oxides and iron oxyhydroxysulfates, which can retain trace elements by coprecipitation and/or sorption processes. The stability of these secondary minerals, which contain high levels of As is of great importance to our understanding of the natural metal(loid) attenuation mechanisms operating in this system.

Introduction

Surface and ground waters near mines of sulfide minerals are often heavily polluted. Waste materials containing residual sulfide minerals are piled up in tailings and may become oxidized producing acid mine drainage (AMD) (Appelo and Postma, 1996). This AMD releases large amounts of metals which remain soluble in the AMD (Appleyard and Blowes, 1994) causing a major environmental issue.

The Tinto Santa Rosa mine (Fig. 1) is located in the Iberian Pyritic Belt (IPB) that is one of the most important metallogenetic provinces of volcanic-hosted massive sulphide deposits in the world (e.g. Leistel et al., 1998). Centuries of mining activity in this area has generated enormous amounts of mining waste, which continue to generate acidity and metal pollution affecting nearby streams and rivers such as the Tinto and Odiel Rivers. The aim of this work is to characterize the mineralogy and chemistry of AMD precipitates and their relationship to the mobility of aqueous trace elements, particularly As, in the acid discharge of the Tinto Santa Rosa mine.
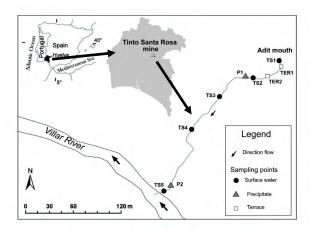

Figure 1. Site map and sampling points in the acid discharge of the Tinto Santa Rosa mine.

Methods

1. Field site and sampling description

All the water and sediment samples described in this study were collected in July of 2006 from the acid discharge of the abandoned Tinto Santa Rosa mine. This shallow stream was studied from the adit mouth to approximately 300 m downstream where it flows into the Villar River (Fig. 1). The stream flows down a narrow channel over terraces of ochreous sediment, forming different terrace levels along the channel. The stream bed is covered with several centimeters of yellowish and reddish precipitates. At each sampling point pH and

temperature were measured and two water samples were taken in acid-pre-washed polyethylene bottles, after rinsing thoroughly with local water. Both samples were filtered through a 0.1-μm pore membrane filter and one sample was acidified with 1 mL of concentrated HNO_3 solution for major and trace element analysis while the other sample was acidified with HCl, adjusting its pH to less than 1, for dissolved Fe(II)/Fe(III) determination. All the water samples were preserved at 4ºC until analyses. Solid samples of the terraces and fresh precipitates were also taken from the surface of the stream bed at depths down to 10 cm at different sampling points. The samples were dried at room temperature for mineralogical determination.

2. Water analysis
The concentration of dissolved major and trace elements were determined by ICP-AES (Thermo Jarrel Ash) and ICP-MS (X-Series II, Thermo), respectively. Ferrous and total dissolved iron concentrations (following reduction with hydroxylamine hydrochloride) were determined by colorimetry using the ferrozine method (modified after To et al., 1999) in a UV-VIS HP spectrophotometer. The concentration of dissolved Fe(III) was taken as the difference between the total concentration of Fe and Fe(II).

3. Sediment characterisation
X-ray diffractometry (XRD) was used to determine the mineralogy of the sediment collected. Each sample, air-dried at room temperature, was ground into a fine slurry. The samples were then analysed using a Bruker D5005 diffractometer with Cu Kα radiation. Powered samples were scanned from 0º to 60º 2θ with a continuous scan at a rate of 0.025º/18s. Samples of precipitates were observed under field-emission scanning electron microscopy (SEM) using a Hitachi H-4100FE with intensity current of 10 kV. The major and trace element content of the sediments was determined using a wavelength dispersion X–ray fluorescence spectrometer (Bruker S4 Explorer). X-ray absorption spectroscopy (XAS) was used to determine the proportion of different Fe phases present and the speciation and local coordination environment of arsenic in the sediments. Arsenic and iron K-edge X-ray absorption spectra were obtained on stations 16.5 and 7.1, respectively, at the CCLRC Daresbury Synchrotron Radiation Source operating at 2 GeV with a beam current of between 130 and 210 mA. Energy resolution was achieved using a Si(220) or Si(111) double crystal monochromator for stations 16.5 and 7.1, respectively, with harmonic contamination of the beam minimised by detuning the second crystal to 70% (16.5) or 50% (7.1). A thin layer of finely ground sediment was mounted in an aluminium sample holder with Sellotape windows. Iron and arsenic data were collected at liquid nitrogen temperature in transmission or fluorescence mode, respectively, with the latter detected using an Ortec 30-element solid state Ge-detector. Further details regarding model compound data collection and data reduction procedures are described by Liu et al. (2006).

Results and Discussion
1. AMD chemistry
Water discharged from the adit mouth is highly acidic, rich in dissolved Fe, SO_4^{2-} and with a noticeable content of trace elements (Table 1).

Table1. Chemical characteristics of Tinto Santa Rosa AMD waters.

		mg L⁻¹											μg L⁻¹					
Sample	pH	SO_4^{2-}	Ca	Cu	Fe $_{TOT}$	Fe (II)	K	Mg	Mn	Si	Zn	Na	As	Cd	Ni	Co	Pb	Sr
TS1	3.42	4026	181	23	996	881	3	145	45	7	85	2	1867	148	616	1101	b.l.	116
TS2	3.01	3375	175	15	656	544	4	100	31	19	57	1	803	99	427	759	76	107
TS3	2.92	3168	218	20	832	538	2	138	42	17	77	2	774	131	576	1026	74	122
TS4	2.80	3034	223	15	587	299	1	101	31	13	56	n.a.	240	91	409	728	55	101
TS5	2.62	2704	180	15	561	234	1	103	31	18	57	n.a.	127	101	458	802	59	103

Upon travelling downstream the pH decreases from 3.4 to 2.6, accompanied by a systematic decrease of ferrous and total iron concentrations, indicating that Fe(II) was oxidized to Fe(III) which, in turn, was removed from the solution by precipitation of oxides and hydroxysulfates of iron such as schwertmannite, goethite and jarosite. The evolution of trace element concentrations downstream shows different patterns. The concentration of Cd and Sr does not change significantly, that of Ni, Cu, Pb and Zn shows only a slightly decrease downstream, while the dissolved As concentration drops systematically as we progress downstream of the adit mouth.
It is known that concentration of trace metals is controlled by adsorption onto mineral surfaces (Stumm, 1992) so the variations in the behaviour of these trace elements can be attributed to the different affinity of each aqueous species to the surface of the precipitates (schwertmannite, goethite and jarosite) assuming (i) there are no other

sources for these elements other than the AMD discharge, and (ii) there are no streams flowing into the Tinto Santa Rosa which may dilute the dissolve metal load.. According to calculations made using the PHREEQC code (Parkhurst and Appelo, 1999) and the WATEQ4F (Ball and Nordstrom, 1991) and MINTEQA2 (Allison et al., 1990) databases, in the pH range of these waters the predominant aqueous species for divalent metals are uncharged complexes (e.g. $PbSO_4^0$) and cationic forms (e.g. Mn^{2+}, Ni^{2+}, Zn^{2+}). These species are likely not adsorbed onto the AMD sediment surface to a sizeable extent since the minerals that make up the bulk of the sediment exhibit a net positive charge at pH ~ 3 (Stumm, 1992), resulting in only the minor changes in the dissolved concentrations of Cd, Ni, Cu, Pb and Zn observed. However, under the oxidising conditions of the site, $H_2AsO_4^-$ would be the thermodynamically stable As species in solution, whose adsorption onto the positively charged surfaces is favoured, resulting in a dramatic drop in the aqueous As concentration with distance from the contaminant point source. These results are in agreement with previous research examining metal(loid) sorption in AMD systems (e.g. Acero et al., 2006; Gault et al., 2005; Sánchez-España, 2005; Lee and Chon, 2006; Fukushi et al., 2003).

2. Mineralogy and chemistry of the AMD precipitates

The sediments collected along the 300 m stretch of the stream are made up of detritic silicates (quartz, illite, kaolinite, feldspars, clinochlore), and oxides and hydroxysulfates of iron such as schwertmannite, jarosite and goethite in the case of the fresh precipitates of the bed of the stream, whereas the upper part of the older, compacted sediments (TER1 and TER2) of the terraces consists of schwertmannite (Fig. 2).
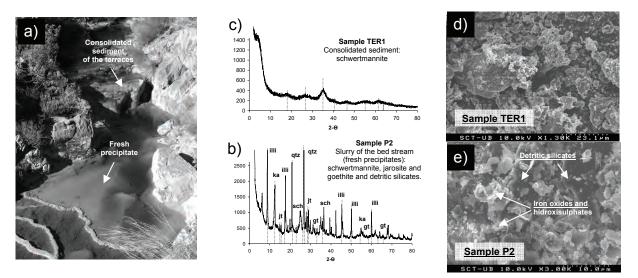
Figure 2. a) View of a sampling point (TS4) and fresh precipitates and terraces of the Tinto Santa Rosa acid discharge (sampling solids); b) and c) XRD diffractograms of the different solids sampled (gt: goethite, qtz: quartz, sch: schwertmannite, illi: illite, ka: kaolinite and jt: jarosite); e) and f) SEM images of the sediments studied.

PHREEQC calculations with the WATEQ4F database were used to estimate the saturation state of the water samples. According to the obtained saturation indexes (SI) the samples are supersaturated with respect to schwertmannite, goethite and jarosite (Table 2), except in TS5 where water is undersaturated with respect to schwertmannite if logK = 18±2.5 is used (Bigham et al., 1996). Although schwertmannite is metastable with respect to goethite, Fukushi et al. (2003) showed that the transformation of schwertmannite to goethite may be retarded and inhibited by sorption of As(V). In our case the consolidated sediments consist of schwertmannite with high As content (TER1 and TER2 in Table 3), and this As enrichment could be responsible for the stability of this Fe-phase.

The arsenic X-ray absorption near edge structure (XANES) spectra obtained from analysis of the fresh precipitate (sample P2) and consolidated sediment of a terrace (sample TER1) indicate that the bulk of the arsenic present in these samples is in its oxidised pentavalent state, although a minor proportion of As(III) was determined in the TER1 sample (Fig. 3a). The best fit of the associated extended X-ray absorption fine structure (EXAFS) spectra was obtained with a first coordination sphere of four oxygen atoms at 1.68 Å, with an outer shell of iron scatterers at 3.30-3.32 Å for both samples, suggesting that the arsenic was associated with an iron mineral assemblage. Pattern fitting of the iron EXAFS data indicated that the iron mineralogy was dominated by

schwertmanite (Fig. 3b.), with lesser amounts of goethite (TER1) and jarosite/goethite (P2) present. While XRD analysis is useful in helping to identify crystalline (and to a lesser extent poorly crystalline) phases, it is of limited use in identifying the proportions of iron assemblages of varying crystallinity. The element specific nature of XAS and its ability to analyse both amorphous and crystalline materials makes it an excellent technique to probe the mineralogy of these complex sediments.

Table 2. Saturation index (SI) calculations using the PHREEQC code and the WATEQ database, with the exception of sch (10.15) (Yu et al., 1999) and sch (18.0) (Bigham et al., 1996).

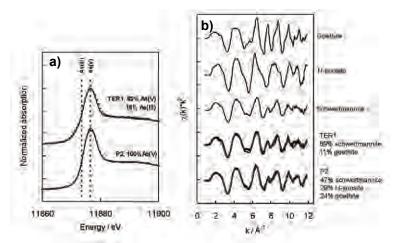| Sample	schwertmannite (10.5)	schwertmannite (18.0)	jarosite-K	jarosite-H_3O	goethite
TS1	16.6	8.6	6.1	2.8	6.1
TS2	9.0	1.1	4.0	1.0	4.9
TS3	11.3	3.3	4.5	1.8	5.2
TS4	8.8	0.8	3.7	1.3	4.9
TS5	6.1	-1.8	2.9	0.7	4.5

Figure 3. a) Arsenic XANES and b) iron EXAFS spectra of sediment samples P2 and TER1 and selected model compounds. Experimental spectra and best fit are displayed as solid and dotted lines, respectively.

The analyses of the aqueous and the solid phase of the system suggest that As-sorption processes could occur. The fresh solid samples show a significant content of trace metals (Mn, Cu, Zn, As and Pb). The evolution of the trace contents in the fresh precipitates downstream (P1 and P2 in Table 3) seems to show that the amounts of Mn, Cu, Zn and Pb do not follow a systematic trend, suggesting that these metals are unlikely to be involved in the sorption processes, while As (the most abundant trace element of both sediments, fresh and consolidated) systematically decreases downstream, mirroring the behaviour of the streamwater As. Nonetheless, collection of further sediment samples is required in order to confirm this trend.

Table 3. Major constituents (wt%) and trace metals (mg g^{-1}) of the solid samples collected based on the X-ray fluorescence results.

| Sample | Major oxides (wt %) | | | | | | | | | | | Trace metals (mg g^{-1}) | | | | |
	Na_2O	MgO	Al_2O_3	SiO_2	P_2O_5	SO_3	K_2O	CaO	TiO_2	Fe_2O_3	As_2O_3	Mn	Cu	Zn	As	Pb
TER 1	-	1.24	0.30	0.69	0.15	12.80	0.03	0.03	-	60.16	3.38	0.06	0.33	0.05	25.60	-
TER2	-	1.06	0.41	0.83	0.12	14.00	0.04	0.03	-	70.09	3.21	-	0.37	0.12	24.30	-
P1	0.40	0.81	17.00	42.90	0.10	6.80	3.13	0.11	0.70	23.02	0.50	0.34	0.60	0.25	3.81	1.86
P2	0.40	0.71	18.30	43.50	0.09	5.91	3.07	0.13	0.70	23.25	0.35	0.30	0.63	0.20	2.62	1.94

Conclusions

The dissolved arsenic content in the acid discharge of the Tinto Santa Rosa mine decreases downstream due to its adsorption onto the surface precipitates of the stream bed (schwertmannite, jarosite and goethite) and onto the consolidated sediment of the terraces (schwertmannite). Although water of Tinto Santa Rosa stream still supplies aqueous arsenic to the Villar River, the As content in the stream decreases from nearly 2000 μg L^{-1} at the mine

adit mouth to just over 100 μg L^{-1} some 300 m downstream. The effectiveness of this natural attenuation of arsenic is clearly dependent on the stability of the iron oxide/hydroxysulfate sorbents, which requires further attention.

Acknowledgements

References

Acero P., Ayora C., Torrentó C., Nieto J.M. (2006). The role of trace elements during schwertmannite precipitation and subsequent transformation into goethite and jarosite. Geochimica et Cosmochimica Acta 70, 4130-4139.

Allison J.D., Brown D.S., Novo-Gradac K.L. (1990). MINTEQA2/PRODEFA2, A Geochemical Assessment Model for Environmental Research Laboratory, Office of Research and Development, U.S. EPA, Athens, GA.

Appelo C.A.J., Postma D. (1996). Geochemistry, groundwaters and pollution. Balkema, Rotterdam.

Appleyard E.C., Blowes D.W. (1994). Application of mass-balance calculations to weathered sulfide mine tailings. In C.N. Alpers and D.W. Blowes (eds), Environmental geochemistry of sulfide oxidation. ACS Symp. Ser. 550, 5169-534.

Ball J., Nordstrom D. (1991). User's manual for WATEQ4F with revised thermodynamic database and test cases for calculating speciation of major, trace and redox elements in natural waters. U.S. Geological Survey Water-Resources Investigation Report 91–183.

Bigham J.M, Schwertmann U., Traina S.J., Winland R.L., Wolf M. (1996). Schwertmannite and the chemical modeling of iron in acid sulfate waters. Geochimica et Cosmochimica Acta 60, 2111-2121.

Gault A.G., Cooke D.R., Townsend A.T., Charnock J.M., Polya D.A. (2005). Mechanisms of arsenic attenuation in acid mine drainage from Mount Bischoff, western Tasmania. Science of Total Environment 345, 219-228.

Fukushi K., Sasaki M., Sato T., Yanese N., Amano H., Ikeda H. (2003). A natural attenuation of arsenic in drainage from an abandoned arsenic mine dump. Applied Geochemistry 18, 1267–1278.

Langmuir D. (1997). Aqueous Environmental Geochemistry. Prentice-Hall, Upper Saddle River.

Lee J.S., Chon H.T. (2006). Hydrochemical characteristics of acid mine drainage in the vicinity of an abandoned mine, Daduk Creek, Korea. Journal of Geochemical Exploration 88, 37-40.

Leistel J.M., Marcoux E., Deschamps Y., Joubert M. (1998). Antithetic behaviour of gold in the volcanogenic massive sulphide deposits of the Iberian Pyrite Belt. Mineralium Deposita 33, 82-97.

Liu W.J., Zhu Y.G., Hu Y., Williams P.N., Gault A.G., Meharg A.A., Charnock J.M., Smith, F.A. (2006). Arsenic sequestration in iron plaque, its accumulation and speciation in mature rice plants (*Oryza Sativa* L.). Environmental Science and Technology 40, 5730-5736.

Parkhurst D.L., Appelo C.A.J. (1999). User's Guide to PHREEQC (Version 2), a computer program for speciation, batch reaction, one-dimensional transport, and inverse geochemical calculations. Water Resources Research Investigations Report 99-4259, 312 pp.

Sánchez-España F.J., López Pamo E., Santofimia E., Reyes J., Martín J. (2005). The natural attenuation of two acidic effluents in Tharsis and La Zarza-Perrunal mines (Iberian Pyrite Belt, Huelva, Spain). Environmental Geology 49, 253-266.

Stollenwerk K.G. (1994). Geochemical interactions between constituents in acidic groundwater and alluvium in an aquifer near Globe, Arizona. Applied Geochemistry 9, 353-369.

Stumm W. (1992). Chemistry of the Soil-Water interaction. Wiley and Sons, New York.

To T.B., Nordstrom D.K., Cunningham K.M., Ball J.W., McCleskey R.B. (1999). New method for the direct determination of dissolved Fe(III) concentration in acid mine waters. Environmental Science and Technology 33, 807-813.

Yu J.Y., Heo B., Choi I.K., Cho J.P., Chang H.W. (1999). Apparent solubilities of schwertmannite and ferrihydrite in natural stream waters polluted by mine drainage. Geochimica et Cosmochimica Acta 63, 3407-3416.